J. Biochem. **143,** 107–115 (2008)
doi:10.1093/jb/mvm196

A Prodigiosin Analogue Inactivates NADPH Oxidase in Macrophage Cells by Inhibiting Assembly of p47phox and Rac

Takuji Nakashima[1,2,*], Takashi Iwashita[3], Tsuyoshi Fujita[3], Emiko Sato[4], Yoshimi Niwano[4], Masahiro Kohno[4], Shunsuke Kuwahara[5], Nobuyuki Harada[5], Satoshi Takeshita[6] and Tatsuya Oda[2]

[1]NITE Biological Resource Center (NBRC), National Institute of Technology and Evaluation (NITE); [2]Division of Biochemistry, Faculty of Fisheries, Nagasaki University; [3]Suntory Institute for Bioorganic Research; [4]New Industry Creation Hatchery Center, Tohoku University; [5]Institute of Multidisciplinary Research for Advanced Materials, Tohoku University; and [6]Joint Research Center, Nagasaki University, Japan

Received August 6, 2007; accepted October 9, 2007; published online October 27, 2007

Prodigiosins are natural red pigments that have multi-biological activities. Recently, we discovered a marine bacterial strain, which produces a red pigment. Extensive two-dimensional nuclear magnetic resonance and mass spectrometry analysis showed that the pigment is a prodigiosin analogue (PG-L-1). Here, we investigated the effect of PG-L-1 on NADPH oxidase activity in macrophage cells. PG-L-1 significantly inhibited superoxide anion (O_2^-) production by phorbol 12-myristate 13-acetate (PMA)-stimulated RAW 264.7 cells, a mouse macrophage cell line. The ED_{50} value was estimated to be ~0.3 μM. PG-L-1 had no direct scavenging effect on O_2^- generated by hypoxanthine/xanthine oxidase system in electron spin resonance-spin trapping determinations, suggesting that this compound directly acts on the O_2^- production system, NADPH oxidase, in macrophage cells. We further investigated the effect of PG-L-1 on the behaviour of the cytosolic components of the NADPH oxidase, $p67^{phox}$, $p47^{phox}$, $p40^{phox}$, Rac and protein kinase C (PKC), in PMA-stimulated RAW 264.7 cells. Although PG-L-1 showed no effect on the activation of PKC, the immunoblotting analysis using specific antibodies showed that PG-L-1 strongly inhibits the association of $p47^{phox}$ and Rac in the plasma membrane of PMA-stimulated RAW 264.7 cells. These results suggest that PG-L-1 inactivates NADPH oxidase through the inhibition of the binding of $p47^{phox}$ and Rac to the membrane components of NADPH oxidase.

Key words: NADPH oxidase inhibitor, prodigiosin, p47phox, Rac protein, superoxide.

Abbreviations: PMA, phorbol 12-myristate 13-acetate; NADPH, nicotinamide adenine dinucleotide phosphate; phox, phagocytic oxidase; phosphate; PKC, protein kinase C; ROS, reactive oxygen species; Nox, NADPH oxidase; phox, phagocytic oxidase; CGD, chronic granulomatous disease; Q-TOF, quadrupole time-of-flight; FT-ICR-MS, Fourier transform ion cyclotron resonance mass spectrometer; TMS, Tetramethylsilane; KRP, Krebs-Ringer-Phosphate; ESR, Electron spin resonance; ESI, electrospray ionization.

Neutrophils and other phagocytic cells play an important role in host defense against microbial infections. The microbicidal mechanism consists of phagocytosis of pathogens, production and subsequent release of reactive oxygen species (ROS) to phagosomes as well as release of bactericidal proteins to phagosomes. During the microbicidal response, professional phagocytic cells such as neutrophils and macrophages produce superoxide anion (O_2^-), a precursor of microbicidal oxidants (*1–3*). The process involves in activation of nicotinamide adenine dinucleotide phosphate (NADPH) oxidase that catalyses the reduction of oxygen molecular to O_2^- at the expense of NADPH in phagocytes. The significance of NADPH oxidase in the host defense is demonstrated by recurrent and life-threatening infections that occur in patients with chronic granulomatous disease, a disorder in which NADPH oxidase is non-functional due to a deficiency in its oxidase components (*4–6*). In addition to its importance in the innate immune system, NADPH oxidase is also a prominent contributor to a variety of inflammatory disorders. The uncontrolled production of ROS intermediates by phagocytic cells may lead to crippling disorders such as shock, inflammation and ischaemia/reperfusion injury (*7*).

NADPH oxidase is a multicomponent enzyme consisting of at least two components bound to plasma membrane ($gp91^{phox}$ and $p22^{phox}$ that together form the flavocytochrome b_{558}), three cytosolic components ($p47^{phox}$, $p67^{phox}$ and $p40^{phox}$) and a small GTPase Rac (*8*). In resting cells, NADPH oxidase is dormant and its components separately exist in the membrane and in the cytosol. When phagocytic cells are exposed to appropriate

*To whom correspondence should be addressed. Tel: +81-438-20-5764, Fax: +81-438-52-2314,
E-mail: nakashima-takuji@nite.go.jp

stimuli, NADPH oxidase is activated to produce O_2^- by association of these cytosolic components with the plasma or phargosome membrane components (*9–12*).

It has been reported that microbial metabolites, such as gliotoxin produced by pathogenic fungi, inhibits the activation of NADPH oxidase (*13–15*), but except gliotoxin there have been few reports on microbial metabolites as NADPH oxidase inhibitors. Exploration of NADPH oxidase inhibitors from microbial metabolites may be important not only in the development of pharmaceutical agents, but also in understanding of infectious processes in which pathogens escape the ROS-based host defense. During our screening of useful bacteria that produce bioactive metabolites from the coastal area of Nagasaki, Japan, we discovered a red-pigmented bacterium, designated as strain MS-02-063 (*16*). In our previous studies, the chemical structural and biochemical analysis revealed that this red pigment belongs to the prodigiosin family, and we named it PG-L-1 (*17*, *18*).

Prodigiosins are a family of naturally occurring red pigments produced by various microorganisms including an opportunistic pathogenic microbe, *Serratia sp*. (*19*). Some members of this family have been reported to exert multiple biological activities such as anti-cancer (*20*, *21*), antimalarial (*22*, *23*), antimicrobial (*24*, *25*), immunosuppressive (*26*, *27*) and DNA cleavage activities (*28*). Although we provided novel evidence that PG-L-1 inhibits the O_2^- production through NADPH oxidase activation in macrophage cell lines (*16*, *17*), the underlying inhibitory mechanisms of this pigment remain to be clarified.

In this study, we investigated the exact structure of PG-L-1 and how the pigment inhibits NADPH oxidase activation by focusing on the translocation of cytosolic NADPH oxidase components to the plasma membrane. Our results suggest that PG-L-1 affects the assembly of not only $p47^{phox}$, but also Rac protein.

MATERIALS AND METHODS

Materials—8-Amino-5-chloro-7-phenylpyrido [3,4-d] pyridazine-1,4-(2H,3H) dione sodium salt (L-012) was from Wako Pure Chemical Industries, Ltd (Osaka, Japan). Xanthine oxidase (XOD from cow milk) and 5,5-dimethyl-1-pyrroline-*N*-oxide (DMPO) were from Labotec Co., Ltd (Tokyo, Japan). Anti-$gp91^{phox}$, anti-$p47^{phox}$, anti-$p67^{phox}$ and anti-$p40^{phox}$ polyclonal antibodies were purchased from Upstate, Serologicals Company (Lake Placid, NY). Anti-Rac 2 polyclonal antibody was from Santa Cruz Biotechnology (Santa Cruz, CA). Molecular markers for SDS–polyacrylamide gel electrophoresis (PAGE) and enhanced chemiluminescence (ECL)-plus reagents were from Amersham Biosciences Corp. (Piscataway, NJ). MESACUP Protein Kinase Assay Kit was from Medical and Biological Laboratories Co., Ltd (Nagoya, Japan). All other reagents were purchased from Sigma unless otherwise specified.

Preparation of PG-L-1—A prodigiosin pigment, PG-L-1, produced by strain MS-02-063 was purified and identified as described previously (*16*, *17*). The maximal PG-L-1 production was achieved by incubation for 40 h at 28°C (*28*). The PG-L-1 was dissolved in methanol at a concentration of 10 mg/mL and stored in the dark at –20°C until use.

Structural determination of PG-L-1—PG-L-1 was finally purified by reversed-phase high-performance liquid chromatography (HPLC: YMC-Pack Pro C18, 10 i.d. × 250 mm, 5 μm, YMC Co., Ltd, Kyoto, Japan) used with the following mobile phase; solution A was 0.01 M ammonium acetate, solution B was 100% methanol. After a 5-min flow with 100% solution A, a 30-min linear gradient to 100% solution B was run at a flow rate of 1 mL/min. The MS analysis was performed on a quadrupole time-of-flight (Q-TOF) mass spectrometer (Micromass, Manchester, UK), which is a hybrid quadropole orthogonal acceleration tandem mass spectrometer, fitted with a Z-spray nano-flow electrospray ion source. Accurate mass of PG-L-1 was measured by use of a Apex-Q94e Fourier transform ion cyclotron resonance mass spectrometer (FT-ICR-MS) (Bruker Daltonik, Bremen, Germany) equipped with a 9.4 T superconducting actively shielded magnet (Magnex Scientific Ltd, Oxford, UK).

NMR spectra were recorded at 25°C in $CDCl_3$ using a AVANCE-750 NMR spectrometer (Bruker BioSpin GmbH, Germany). Tetramethylsilane [TMS: $Si(CH_3)_4$] was used as the chemical-shift reference for both proton and carbon-13. The assignments of the proton and carbon-13 resonances at the chemical structure of PG-L-1 were based on the two-dimensional $^1H\{^{13}C\}$-HSQC, $^1H\{^{13}C\}$-HMBC, DQF-COSY, TOCSY, NOESY spectra and the chemical shifts values.

Cell Culture—RAW 264.7 cells, a mouse macrophage cell line obtained from the American Type Culture Collection (Rockville, MD, USA) were cultured in RPMI 1640 medium supplemented with 10% fetal bovine serum, penicillin G (100 U/mL) and streptomycin (100 U/mL) as described previously (*16*). The adherent cells in the flasks were washed twice with phosphate-buffered saline. The cells were subsequently scraped with a cell scraper (Becton Dickinson), and were harvested by centrifugation at 1,000×*g* for 5 min at 4°C.

Measurement of Superoxide—In the chemiluminescence analysis for the detection of O_2^- produced by RAW 264.7 cells, we employed L-012 (Wako Chemical), which is a highly sensitive chemiluminescence probe for analysing ROS (*29*). Krebs–Ringer–Phosphate (KRP) buffer with 11 mM glucose containing 10^5 cells and 10 μM L-012 were prepared in each well of a 96-well microtitre plates. To the cell suspension of 180 μL, 10 μL of PG-L-1 dissolved in methanol (at final concentrations ranging from 0 to 100 μM), superoxide dismutase dissolved in KRP buffer (SOD, at a final concentration of 10 U/200 μL) or staurosporine dissolved in dimethyl sulfoxide (DMSO) (protein kinase C inhibitor, at a final concentration of 0.1 μM) were added, and the resultant mixture was then incubated for 3 min at 37°C. After incubation, the reaction was started by addition of 10 μL of 2 μM phorbol 12-myristate 13-acetate (PMA) dissolved in DMSO. During the incubation, chemiluminescence emission was recorded continuously for 15 min by using multilabel recorder Mithras LB940 (Berthold Technologies GmbH and Co. KG., Bad Wildbad, Germany).

Electron Spin Resonance (ESR)-Spin-Trapping Determinations for Superoxide Produced by Hypoxanthine (HPX)-Xanthine Oxidase (XOD) Cell-Free System—In the presence of a spin-trapping agent, DMPO, O_2^- reacts with DMPO to yield a more stable spin adduct, DMPO-OOH. In brief, 50 μL of 2 mM HPX dissolved in 0.1 M phosphate buffer (PB), 30 μL of DMSO and 50 μL of PG-L-1 [up to a concentration of 200 μg/mL (56.9 μM)] or methanol (vehicle) alone, 20 μL of 4.5 M DMPO dissolved in pure water, and 50 μL of 0.4 U/mL XOD dissolved in 0.1 M PB were placed in a test tube and mixed. In the reaction mixture, to eliminate the effect of hydroxyl radical, DMSO was added as a hydroxyl radical-scavenger. The mixture was transferred to an ESR spectrometry cell, and the DMPO-OOH spin adduct was quantified 97 s after the addition of XOD. ESR spectrum of DMPO-OOH signal was measured with an ESR spectrophotometer (JES-FA100; JEOL, Tokyo, Japan), operating at a microwave power of 4 mW, a modulation amplitude of 0.07 mT, a time constant of 0.03 s and sweep width of 335.5 ± 5 mT, sweep time of 2 min. Cu, Zn-SOD was used as a standard inhibitor of DMPO adduct formation because a decrease in DMPO-OOH signal intensity correlated with the SOD concentrations.

Separation of Whole Cell Protein into Triton X-100-Soluble (Cytosol) and -Insoluble (Cytoskeleton) Fractions—When PMA-activated neutrophils were separated by treatment with Triton X-100 into detergent-soluble and detergent-insoluble fractions (defined as the cytoskeleton), cytosolic NADPH components were mainly associated with the cytoskeleton fraction (*30*). The effects of PG-L-1 on cytoskeletal localization of cytosolic NADPH components were performed as described previously (*31*) with some modifications. In brief, confluent RAW 264.7 cells were washed twice in ice-cold phosphate-buffered saline and detached by scratching. Cells (2×10^7/mL) were incubated for 10 min at 37°C in the presence of 10 μL of PG-L-1 dissolved in methanol (at final concentrations ranging from 0 to 10 μM) and 10 μL of PMA dissolved in DMSO (at a final concentration of 100 ng/mL) or 10 μL of DMSO. After incubation, the cell suspension was harvested by centrifugation (at 1,000 × *g* for 5 min) and then suspended in extraction buffer (pH 7.4) containing 10 mM HEPES, 120 mM NaCl, 5 mM KCl, 10 mM glucose, 1mM phenylmethyl sulfonyl fluoride, 0.1 mM EDTA, 10 μM leupeptin, 10 μM pepstatin and 2% Triton X-100. The cells were disrupted using a microprobe sonicator three times for 10 s each on ice. The Triton X-100-soluble and -insoluble fractions were separated by centrifugation at 21,000 × *g* for 15 min. The supernatant (cytosolic fraction) was transferred to a new tube, and the pellet (cytoskeletal fraction) was washed with the extraction buffer to eliminate the residual soluble elements. The cytoskeletal fraction was then resuspended in 100 μL of 3-[*N*-morpholino]propanesulfonic acid (MOPS)-KOH buffer, and the protein concentration was determined by the method described by Lowry *et al*. (*32*) using bovine serum albumin as a standard. After addition of 400 μM NADPH dissolved in KRP buffer, NADPH-responsible O_2^- production activity of this cytoskeletal fraction (100 μg) was measured at 37°C for 15 min by L-012-mediated chemiluminescence assay. In addition, aliquots of protein samples (50 μg each) were boiled in SDS buffer for immunoblotting.

Concentrations of PG-L-1 in Subcellular Fractions of RAW 264.7 Cells—To investigate the accumulation of PG-L-1 into subcellular fractions in RAW 264.7 cells, cytosolic and plasma membrane fractions were prepared as described previously (*33*) with some modifications. Because PG-L-1 bound to the cytoskeletal fraction was easily extracted by a detergent, Triton X-100 method was unsuitable for this accumulation test. PG-L-1 dissolved in methanol (at final concentrations ranging from 0 to 10 μM) was added to the cell suspension of RAW 264.7 in KRP buffer (1×10^7 cells/0.5 mL) in a 1.8-mL centrifuge tube. The tubes were incubated at 37°C for 5 min. The cells were then collected by centrifugation (at 1,000 × *g* for 5 min) and washed twice with KRP buffer. The cell suspension was harvested by centrifugation (at 1,000 × *g* for 5 min) and then suspended in 0.5 mL of relaxation buffer containing 10 mM Pipes, pH 7.4, 100 mM KCl, 3 mM NaCl, 3.5 mM $MgCl_2$, 1 mM phenylmethyl sulfonyl fluoride, 0.1 mM EDTA, 10 μM leupeptin and 10 μM pepstatin. The cells were disrupted using a microprobe sonicator three times for 10 s each on ice. The soluble and insoluble fractions were separated by centrifugation at 100,000 × *g* for 30 min at 4°C. The supernatant (cytosolic fraction) was transferred from subcellular fractions to a new tube, and the pellet (plasma membrane fraction) was washed with the relaxation buffer and separated by centrifugation at 100,000 × g for 30 min at 4°C. PG-L-1 bound to membrane was extracted by methanol (0.5 mL). The concentrations of PG-L-1 in the cytosolic and plasma membrane fractions were measured by using reversed-phase HPLC. In HPLC, ODS C-18 column (4.6 i.d. × 250 mm, Finepak SIL 300C18T-7 JASCO, Tokyo, Japan) was used with the following mobile phase; solution A was 0.01 M ammonium acetate, solution B was 100% methanol. After a 5-min flow with 100% solution A, a 30-min linear gradient to 100% solution B was run at a flow rate of 1 mL/min. Analysis of PG-L-1 were performed with three-dimensional chromatogram by Millennium^{32} PDA Software (Waters Co., Milford, Mass., USA) (*16*).

Assay for Protein Kinase C (PKC) Activity—The cytosolic and cytoskeletal fractions were prepared by Triton X-100 method as described earlier. RAW 264.7 cells were treated with PG-L-1 (at a final concentration of 10 μM) and/or PMA (at a final concentration of 100 ng/mL) for stimulation and translocation of PKC to the cytoskeletal fraction. PKC activity was measured by using a non-radioactive protein kinase assay kit (MESACUP Protein Kinase Assay Kit; Medical and Biological Laboratories Co., Ltd, Nagoya, Japan). This assay kit was based on the enzyme-linked immunosorbent assay that consists of synthetic PKC pseudosubstrates and monoclonal antibody against the phosphorylated peptide. PKC phosphorylates serine of the pseudosubstrate through a Ca^{2+}/phosphatidylserine-dependent mechanism. PKC activity of the plasma membrane fraction was assayed in the presence of Ca^{2+} and phosphatidylserine, and the negative control was measured in the presence of 20 mM EGTA alternative

to phosphatidylserine. Data are expressed as $OD_{492}/12\,\mu L$ cell lysate from 2×10^7 cells.

Immunoblot Analysis—Western blotting analysis using rabbit polyclonal antibodies against $gp91^{phox}$, $p47^{phox}$ $p67^{phox}$, $p40^{phox}$ and Rac 2, and peroxidase-conjugated goat anti-rabbit IgG antibody (Upstate Biotechnology) was performed for probing each protein according to the usual procedure. The membrane fractions were resuspended in 5% SDS sample buffer containing 100 mM dithiothreitol and then boiled for 5 min at 100°C. Aliquots of protein samples (50 μg each) were subjected to SDS–PAGE (12.5% gel). The separated proteins were then transferred to a PVDF membrane. After being blocked with 5% (w/v) skin milk in phosphate-buffered saline containing 0.1% (w/v) Tween 20, the separated proteins were probed with the respective primary antibodies, followed by probing with horseradish peroxidase-conjugated secondary antibody (Upstate Biotechnology). Their immunoreactive bands were visualized with enhanced chemiluminescence-plus reagents (Amersham).

Statistical Analysis—Data are expressed as the mean ± standard deviation (SD). Individual treatment groups were compared with appropriate controls using Dunnett's multiple comparison test. A difference was considered significant at $P < 0.05$.

RESULTS

Identification of PG-L-1—The isolated pigment compound, PG-L-1, showed maximal absorption at 535 nm. The positive ESI-Q-TOF-MS spectrum of PG-L-1 showed an intense peak at *m/z* 352 (Fig. 1C). The molecular formula of PG-L-1 was established as $C_{22}H_{29}N_3O$ by FT-ICR-MS (ESI) analysis [*m/z* 352.23849 $(M + H)^+$, (Δ −0.4 mmu)]. The NMR spectra of the purified pigment summarized in Table 1 indicate that the pigment compound is a prodigiosin analogue. The reported carbon-13 chemical shifts of prodigiosin hydrochloride (*34*) were very similar to those of PG-L-1. These facts indicate that the pigment was a close derivative of prodigiosin. Moreover, according to the Q-Tof MS/MS results, a major peak at *m/z* 252 was observed in PG-L-1 (Fig. 1D). It is suggested that the addition of ethylene to the pentyl chain of prodigiosin (Fig. 1B) forms PG-L-1 (Fig. 1A). Thus, the gross structure of PG-L-1 was elucidated to be 2-methyl-3-heptyl-6-methoxyprodigiosene.

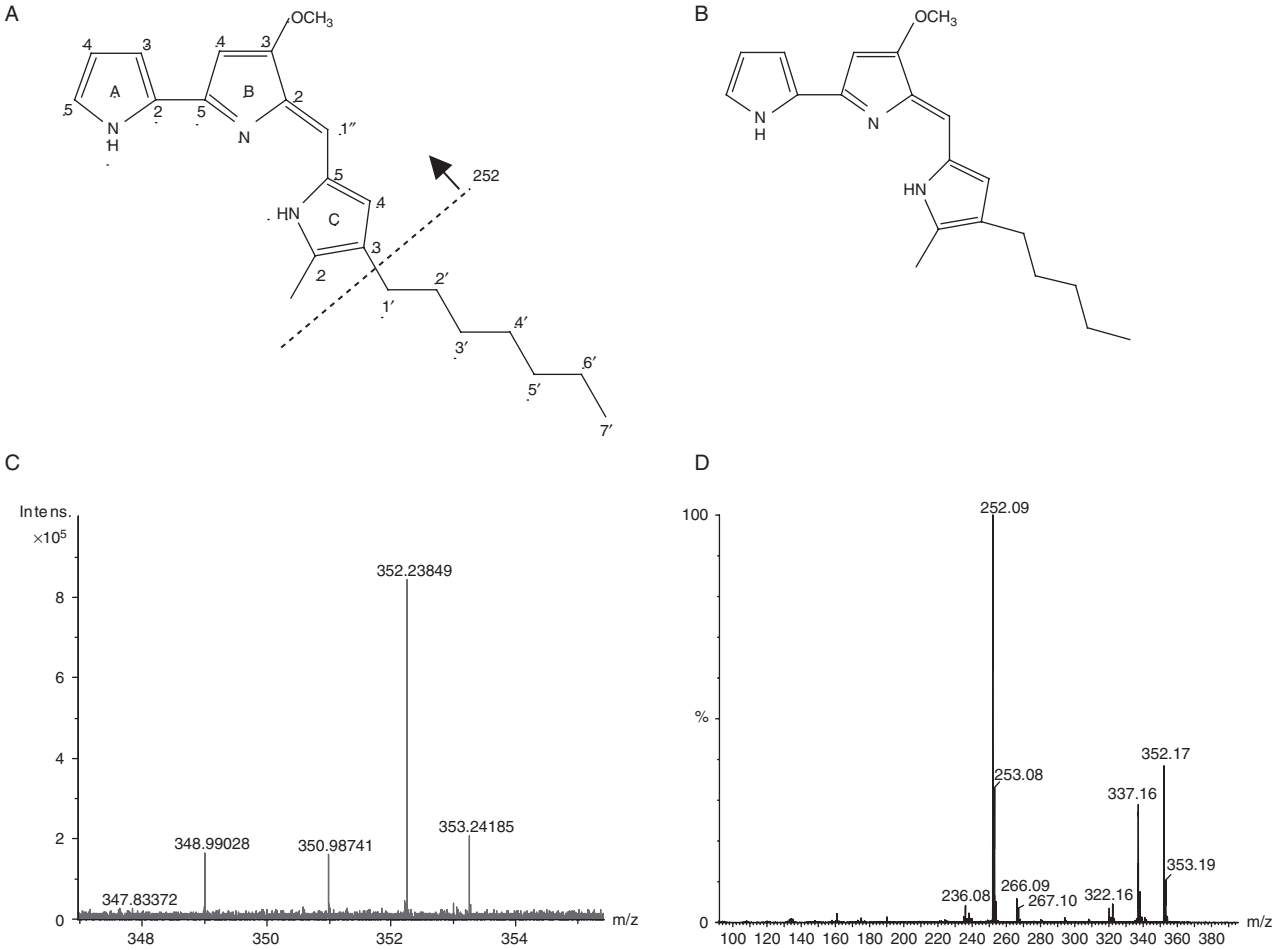

Fig. 1. **Structures of prodigiosin members.** (A) PG-L-1 from strain MS-02-063. (B) Prodigiosin (Ref. 28). (C) Positive ESI-Q-TOF-MS spectrum of PG-L-1. (D) Time-of-flight MS/MS spectrum of PG-L-1. The product ion (*m/z* 252) that is estimated detachment of methylene chain from PG-L-1 was observed.

Table 1. **Proton and carbon-13 chemical shifts of PG-L-1 and prodigiosin.**

No.	PG-L-1 Carbon (δ ppm)	Proton (δ ppm)	Prodigiosin HCl Carbon (δ ppm)
A2	122.3		121.9
A3	117.0	6.932	117.0
A4	111.8	6.366	111.5
A5	127.1	7.247	126.2
B2	120.7		120.5
B3	165.9		165.5
B4	92.8	6.095	92.7
B5	147.6		147.4
C2	128.5		146.0
C3	147.1		128.0
C4	128.5	6.692	128.0
C5	125.3		124.8
1″	116.0	6.968	8.4
Alkyl			
OCH3	58.7	4.018	58.5
1′	25.3	2.396	25.0
2′	30.0	1.536	29.4
3′	29.2	1.316	31.2
4′	29.7	1.255	
5′	31.9	1.271	
6′(4′)	22.8	1.297	22.2
7′(5′)	14.2	0.888	13.7
C_2Me	12.8	2.533	12.0

NMR spectra were recorded at 25°C in $CDCl_3$ using AVANCE-750 spectrometer ($_1$H resonance frequency: 750.013 MHz). TMS was used as the chemical shift reference for both proton and carbon-13. The assignments of the proton and carbon-13 resonances at the chemical structure of PG and PG-L-1 were based on the two-dimensional $^1H\{^{13}C\}$-HSQC, $^1H\{^{13}C\}$-HMBC, DQF-COSY, TOCSY, NOESY spectra and the chemical shifts values. In the table, the reported carbon-13 chemical shift values of prodigiosin were also shown as the values from TMS. (The reported values were measured based on the reference of CHCl3 which was 80 ppm. The values were corrected by substracting 2.78 ppm from the reported values.) The reported carbon 1″ value of prodigiosin hydrochloride was seemed to be a typographical error. The carbon-13 assignment of C2 and C3 should be replaced each other from the data of the long range spin-spin coupling constants between the protons and carbons related to C2 and C3 which were measured by $^1H\{^{13}C\}$-J-HMBC.

Effect of PG-L-1, a Prodigiosin Pigment, on O_2^- Production by PMA-Stimulated RAW 264.7 Cells—Initially we examined the effects of a prodigiosin analogue, PG-L-1 (Fig. 1A), on PMA-stimulated O_2^- production. The L-012-mediated chemiluminescence method was employed for the detection of O_2^- production by RAW 264.7 cells. SOD (10 U/200 μL) inhibited the chemiluminescence response by ~75% in PMA-stimulated RAW 264.7 cells. When RAW 264.7 cells were treated with PG-L-1, the PMA-stimulated O_2^- production was dose-dependently reduced (Fig. 2). The magnitude of inhibition at 1 μM of PG-L-1 was comparable with that given by 10 U of SOD.

Effect of PG-L-1 on O_2^- Production by HPX/XOD System—Scavenging ability of PG-L-1 against O_2^- was measured by ESR in HPX/XOD-dependent O_2^- production system. SOD showed O_2^- scavenging ability in an activity-dependent manner, whereas PG-L-1 had no scavenging effect even at the highest concentration (56.9 μM) (Fig. 3). This result raised the possibility that PG-L-1 inhibited the activation of NADPH oxidase,

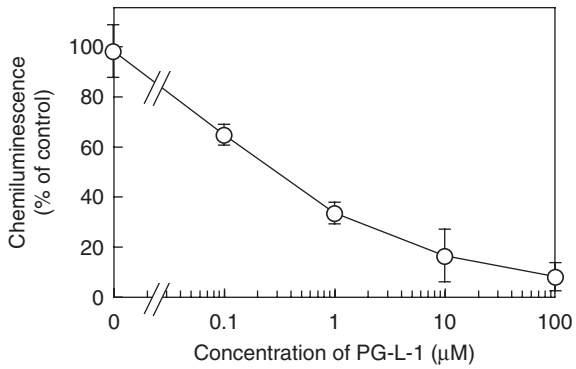

Fig. 2. **Effect of PG-L-1 on O_2^- production in macrophage cells.** PG-L-1 inhibited O_2^- production by PMA-stimulated RAW 264.7. NADPH-dependent O_2^- production by PMA-stimulated RAW 264.7 cells was measured by L-012-mediated chemiluminescence ($n = 5$).

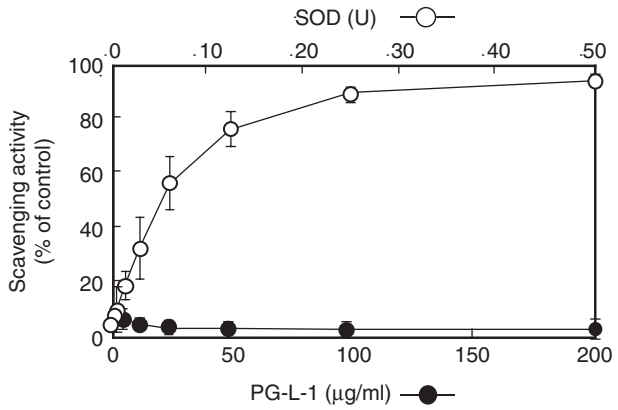

Fig. 3. **Scavenging effect of PG-L-1 on O_2^- production by hypoxanthine/xanthine oxidase system.** O_2^- scavenging activity of PG-L-1 or SOD as measured by the ESR-spin trapping method. PG-L-1 (200 μg/mL is equivalent to 56.9 μM) had no direct scavenging effect on O_2^- production by hypoxanthine/xanthine oxidase system. Results represent the mean ± SD ($n = 3$).

which catalysed the production of O_2^- from oxygen molecular and NADPH, in RAW 264.7 cells. Therefore, we focused on the inhibitory mechanisms of NADPH oxidase activation by PG-L-1.

Binding of PG-L-1 to plasma membrane in RAW 264.7 cells—We examined whether PG-L-1 was accumulated in the intracellular compartments or bound to the plasma membrane in RAW 264.7 cells. The intracellular levels of PG-L-1 were constantly as low as ~0.1 μg/10^7 cells at the concentrations ranging from 1 to 100 μM, whereas the PG-L-1 levels bound to the plasma membrane were significantly increased with the concentrations of PG-L-1 (Fig. 4).

Activity of NADPH Oxidase in Cytoskeleton Fractions—A cytoskeleton fraction separated by Triton X-100 from PMA-stimulated RAW 264.7 cells pretreated with PG-L-1, as an experimental system for the NADPH-dependent O_2^- producing activity, were prepared, and the NADPH oxidase activity was determined by L-012-mediated chemiluminescence assay. As shown in Fig. 5, the NADPH oxidase activity of the cytosol fraction

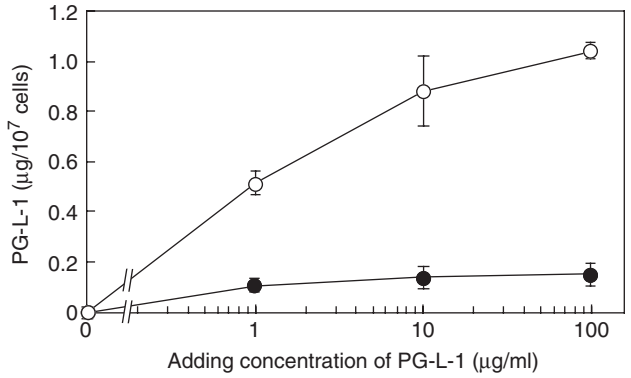

Fig. 4. **Subcellular localization of PG-L-1 in RAW 264.7 cells.** Localization of PG-L-1 to the plasma membrane (open circles) and intracellular fractions (closed circles) expressed as concentrations of PG-L-1 for 10^7 cells ($n=3$ separate measurements). The concentrations of PG-L-1 were primarily increased in the plasma membrane fraction in a time- and concentration-dependent manner but not in the intracellular fraction. Results represent the mean ± SD ($n=3$). $^*P<0.01$ versus intracellular fraction values.

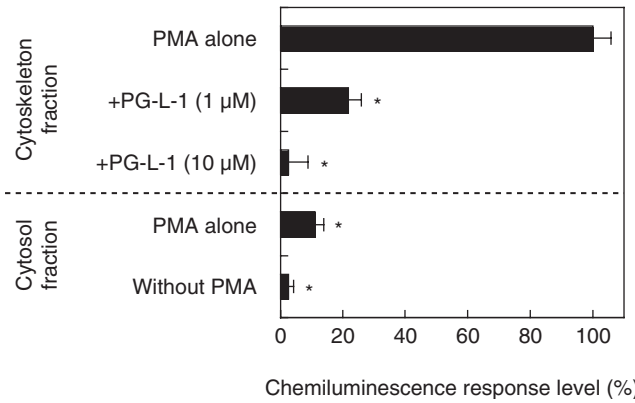

Fig. 5. **Effect of PG-L-1 on subcellular NADPH oxidase activity.** PG-L-1 was added to RAW 264.7 cells (2×10^7 cells/mL), subsequently stimulated with PMA for 10 min at 37°C, and finally, their cytoskeleton fractions were fractionated as described under 'Experimental Procedures'. Production of O_2^- was initiated by addition of NADPH to the cytoskeletal fraction aliquots. NADPH oxidase activity was measured as the intensity of L-012-dependent chemiluminescence. Results represent the mean ± SD ($n=3$). $^*P<0.01$ versus PMA alone.

treated with PMA and the cytoskeleton fraction treated without PMA showed 11 ± 2.7 and 2.5 ± 1.7%, respectively, as compared with that in the cytoskeleton fraction control (PMA alone). The activation of NADPH oxidase by PMA stimulation was significantly inhibited by the pretreatment with PG-L-1 in a concentration-dependent manner. These results suggest that the inhibitory process of PG-L-1 is associated with NADPH oxidase activation such as translocation of cytosolic phox components to the plasma membrane at the cellular level.

Effect of PG-L-1 on Activation of Protein Kinase C—ROS production by macrophages depends on the assembly of cytosolic and membrane-associated components to activate NADPH oxidase through a process regulated by PKC (*35*). Therefore, to investigate the mechanism by which PG-L-1 inhibits O_2^- production by

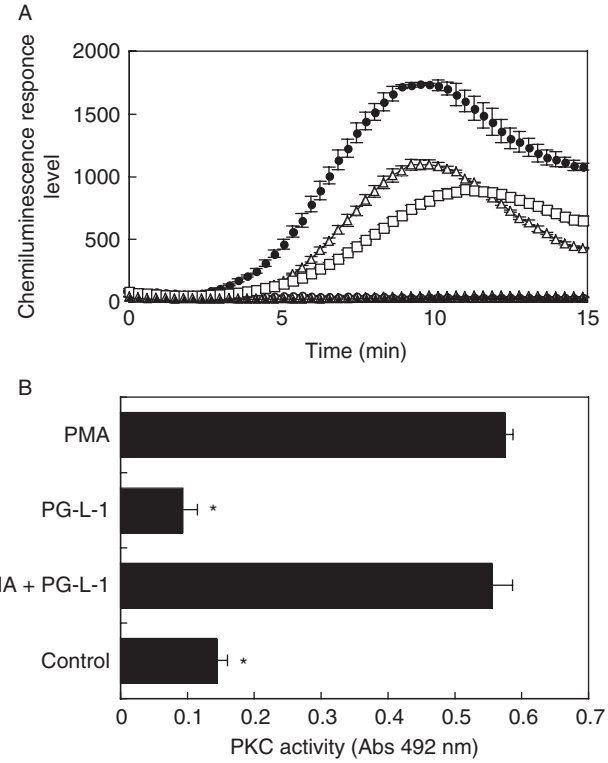

Fig. 6. **Effect of PG-L-1 on the translocation of PKC to the plasma membrane.** (A) The effect of PG-L-1 and staurosporine on O_2^- production by PMA-stimulated RAW 264.7 cells. PMA alone (closed circles), PMA plus 1 μM of PG-L-1 (open triangles), PMA plus 0.1 μM of staurosporine (open squares), PMA plus 1 μM of PG-L-1 and 0.1 μM of staurosporine (open circles), PMA free (closed triangles). The synergistic effect of PG-L-1 and staurosporine on PMA-stimulated O_2^- production was observed. Results represent the mean ± SD ($n=3$). (B) The direct effect of PG-L-1 on PKC. PMA and PG-L-1 was performed at a final concentration of 100 ng/mL and 10 μM, respectively, as described under 'Experimental Procedures'. PG-L-1 alone is equivalent for negative control. PG-L-1 has no effect on translocation of PKC to the membrane. Results represent the mean ± SD ($n=3$). $^*P<0.01$ versus PMA alone.

PMA-stimulated RAW 264.7 cells, we analysed the effect of PG-L-1 on the translocation of PKC to the membrane. As shown in Fig. 6A, the inhibitory activity of 1 μM of PG-L-1 against the O_2^- production by PMA-stimulated RAW 264.7 cells was equivalent to that given by 0.1 μM of staurosporine, and PG-L-1 and staurosporine had synergistic effect on the O_2^- production. Next, we investigated whether PG-L-1 affects the PKC activity using MESACUP Protein Kinase Assay Kit. The high levels of PKC activity were observed in the cytoskeletal fraction of the PMA-stimulated RAW 264.7 cells. Under the same conditions, PG-L-1 had no effect on the translocation of PKC by PMA (Fig. 6B).

Effects of PG-L-1 on assembly of cytosolic phox components and Rac—In resting macrophage cells, the three cytosolic phox components ($p67^{phox}$, $p47^{phox}$ and $p40^{phox}$), and low-molecular-weight Rac protein are located only in the cytosol (*8*). The stimulation by PMA causes the membrane translocation of these phox components and Rac 2 in macrophage cells (*36–38*). As shown in Fig. 7, expressions of $p67^{phox}$, $p40^{phox}$ and Rac

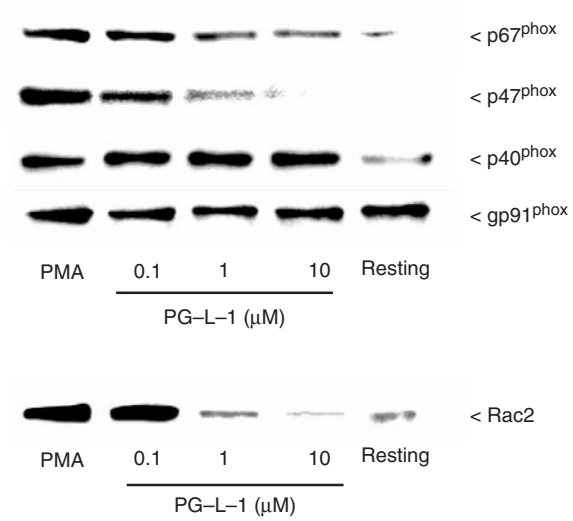

Fig. 7. **Western blot analysis of cytosolic NADPH oxidase components in RAW 264.7 cells.** RAW 264.7 cells were incubated in the absence or presence of PMA (100 ng/mL) and PG-L-1 (at final concentrations of 0.1, 1 and 10 μM) for 10 min at 37°C. Each sample of the plasma membrane fractions was prepared and the membrane associated cytosolic NADPH oxidase components was detected by Western blotting. The samples of plasma membrane fractions were separated by 12.5% SDS–PAGE and western blotting was done with antibodies (1:2000) specific for $gp91^{phox}$, $p47^{phox}$ $p67^{phox}$, $p40^{phox}$ and Rac 2 as described under 'Experimental Procedures'.

were slightly observed in resting cells, and the three phox components ($p67^{phox}$, $p47^{phox}$ and $p40^{phox}$) and Rac were clearly upregulated in the plasma membrane fraction of PMA-stimulated RAW 264.7 cells. The upregulated expressions of $p67^{phox}$, $p47^{phox}$ and Rac in the cytoskeleton fraction were suppressed by the treatment at the indicated concentrations of PG-L-1.

DISCUSSION

Through our extensive screening for useful bacteria from the coastal area of Nagasaki, Japan, we discovered a red-pigmented bacterium, designated as a strain MS-02-063. The strain MS-02-063 was phylogenetically closely related to *γ-proteobacterium* MBIC 3957 from 16S rRNA sequence analysis; however, there were differences in the physiological and biochemical properties (*16*). The red pigment produced by the strain MS-02-063 had multi bioactivities such as antifungal, antibacterial, tumoricidal, and algicidal activities *in vitro* (*16–18*, *23*, *39*). The structure of PG-L-1 was elucidated by extensive two-dimensional NMR techniques including ^{1}H-^{13}C HSQC and HMBC analysis and MS analysis, suggesting that its structure is an adduct of C_2H_4 to the pentyl chain of prodigiosin (Fig. 1, Table 1). We have demonstrated at the cellular level that a prodigiosin member, PG-L-1, interferes with the respiratory burst, which is induced by PMA, of macrophages (RAW 264.7 cell line) [(*16*, *40*), see Fig. 2] and monocytes (U937 cell line) (*17*). However, the underlying mechanism, by which PG-L-1 interferes with the respiratory burst, remains to be elucidated. In the present study, we investigated the mechanism(s) by which PG-L-1 inhibits O_2^- production through activation of NADPH oxidase in RAW 264.7 cells.

PG-L-1 suppressed O_2^- production by PMA-stimulated RAW 264.7 cells in a concentration-dependent manner (Fig. 2), but did not scavenge O_2^- (Fig. 3). As shown in Fig. 4, PG-L-1 significantly accumulated in plasma membrane but not in intracellular compartment of macrophages during the indicated measurement times, suggesting that PG-L-1 bound to the plasma membrane is responsible for the inhibition of O_2^- production. In addition, we showed here that PG-L-1 directly interfered with the NADPH oxidase-induced O_2^- production in the cell-free activation assay (Fig. 5) as well as in the primed cells treated with PMA. These results suggest that PG-L-1 bound to the plasma membrane inhibits the activation of NADPH oxidase and interferes with the translocation of cytosolic NADPH oxidase components to the membrane.

The phosphorylation of $p47^{phox}$ and subsequent O_2^- production by the assembled NADPH oxidase components can be induced by PMA, a potent activator of PKC, and the induction is prevented by PKC inhibitors such as staurosporine (Ref. 41, see Fig. 6A). Hence, we examined the effect of PG-L-1 on PKC. The inhibition rates at 1 μM of PG-L-1 and 0.1 μM of staurosporine against the PMA-stimulated O_2^- production were 38.1 ± 1.6 and $51.6 \pm 4.2\%$, respectively, as compared with the level of inhibitor-free control. Intriguingly, the combination of these compounds allowed almost complete inhibition against the O_2^- production (Fig. 6A). It is possible that PG-L-1, like staurosporine, interferes with the PMA-stimulated O_2^- production through inhibition of PKC activity. Therefore, we examined the effect of PG-L-1 on translocation of PKC to the membrane by using non-radioactive protein kinase assay kit. As shown in Fig. 6B, PMA-induced activation of PKC was not affected by the addition of PG-L-1 to the cells. There is a possibility that the data only shows the effect of PG-L-1 on the translocation of PKC from the cytosolic compartment to the plasma membrane. However, since PG-L-1 accumulates in the plasma membrane (Fig. 4) and PKC mediates phosphorylation of $p47^{phox}$ in the cytosolic compartment (*8*), PG-L-1 unlikely interferes with the activity of PKC in the cytosolic compartment and following translocation to the plasma membrane. Therefore, it is suggested that PG-L-1 directly reacts with NADPH oxidase components in the plasma membrane. We further investigated the effect of PG-L-1 on the assembly of three cytosolic phox components and Rac by using Western blotting analysis. We found that PG-L-1 strongly inhibited the translocation of $p47^{phox}$ and Rac from the cytoplasm to the plasma membrane during NADPH oxidase activation (Fig. 7).

As shown in Fig. 7, PG-L-1 strongly inhibited the expression of $p47^{phox}$ in the plasma membrane in PMA-stimulated cells in a concentration-dependent manner. In contrast, a slight decrease in the expression of $p67^{phox}$ was observed in the plasma membrane of PMA-stimulated RAW 264.7 cells treated with PG-L-1. In addition, PG-L-1 had no effect on $p40^{phox}$ that has a PX domain that specifically binds to phosphatidylinositol 3-phosphate (*42*, *43*). Thus, $p40^{phox}$ is also thought to

serve as an adaptor component that recruits $p67^{phox}$ to the plasma membrane (*44*). It has been reported that the cytoplasmic phox proteins exist as a stable ternary cytoplasmic complex ($p47^{phox}$–$p67^{phox}$–$p40^{phox}$) in a dephosphorylated state. From our results, it is conceivable that the translocation of ternary cytoplasmic complex to the plasma membrane in the primed cells treated with PG-L-1 may be achieved; however, PG-L-1 may specifically eliminate $p47^{phox}$ from the associated membrane. Therefore, $p67^{phox}$ without the support of $p47^{phox}$ may be barely retained in the plasma membrane because only $p40^{phox}$ functions as another adaptor (*45*). It is likely that the inhibitory action of PG-L-1 is to eliminate $p47^{phox}$ from the plasma membrane.

The translocation of Rac to the membrane was also inhibited by PG-L-1 (Fig. 7). Upon activation of NADPH oxidase by PMA, and possibly under the influence of lipid mediators (*46*), Rac dissociates from guanosine diphosphate dissociation inhibitor (refer to as GDI), allowing GTP-bound Rac to translocate to the plasma membrane (*47*, *48*). At the plasma membrane, Rac in the GTP-bound state directly interacts with $p67^{phox}$ via binding to the N-terminal domain that harbors tetratricopeptide repeat (refer to as TPR) motifs (*49*, *50*), and thus the Rac-$p67^{phox}$ complex supports NADPH oxidase activity, leading to O_2^- production (*51*, *52*). PG-L-1 may eliminate Rac from the plasma membrane as well as that of $p47^{phox}$, inhibit the binding of Rac and membrane or interfere with the influence of lipid mediators on Rac. Although the exact action of PG-L-1 on NADPH oxidase assembly is still unclear, PG-L-1-treated cells seem to fail to activate the NADPH oxidase by inhibiting the assembly of not only $p47^{phox}$ but also Rac (Fig. 7).

In summary, our results suggest that PG-L-1, a prodigiosin pigment, affects the translocations of $p47^{phox}$ and Rac to the plasma membrane during NADPH oxidase activation, resulting in that PG-L-1 inhibits NADPH oxidase activation in PMA-stimulated macrophage cells.

We are grateful to Dr Yoshiyuki Itoh (Suntory Institute for Bioorganic Research) for FT-ICR MS analysis.

REFERENCES

1. Cross, A.R. and Jones, O.T. (1991) Enzymic mechanisms of superoxide production. *Biochim. Biophys. Acta.* **1057**, 281–298
2. Babior, B.M. (1992) The respiratory burst oxidase. *Adv. Enzymol. Relat. Areas. Mol. Biol.* **65**, 49–95
3. Chanock, S.J., el Benna, J., Smith, R.M., and Babior, B.M. (1994) The respiratory burst oxidase. *J. Biol. Chem.* **269**, 24519–24522
4. Smith, R.M. and Curnutte, J.T. (1991) Molecular basis of chronic granulomatous disease. *Blood* **77**, 673–686
5. Roos, D., de Boer, M., Kuribayashi, F., Meischl, C., Weening, R.S., Segal, A.W., Ahlin, A., Nemet, K., Hossle, J.P., Bernatowska-Matuszkiewicz, E., and Middleton-Price, H. (1996) Mutations in the X-linked and autosomal recessive forms of chronic granulomatous disease. *Blood* **87**, 1663–1681
6. Lekstrom-Himes, J.A. and Gallin, J.I. (2000) Immunodeficiency diseases caused by defects in phagocytes. *N. Engl. J. Med.* **343**, 1703–1714
7. Cuzzocrea, S., Riley, D.P., Caputi, A.P., and Salvemini, D. (2001) Antioxidant therapy: a new pharmacological approach in shock, inflammation, and ischemia/reperfusion injury. *Pharmacol. Rev.* **53**, 135–159
8. Babior, B.M. (1999) NADPH oxidase: an update. *Blood* **93**, 1464–1476
9. Inanami, O., Johnson, J.L., and Babior, B.M. (1998) The leukocyte NADPH oxidase subunit p47PHOX: the role of the cysteine residues. *Arch. Biochem. Biophys.* **350**, 36–40
10. Inanami, O., Johnson, J.L., McAdara, J.K., Benna, J.E., Faust, L.R., Newburger, P.E., and Babior, B.M. (1998) Activation of the leukocyte NADPH oxidase by phorbol ester requires the phosphorylation of p47PHOX on serine 303 or 304. *J. Biol. Chem.* **273**, 9539–9543
11. Johnson, J.L., Park, J.W., Benna, J.E., Faust, L.P., Inanami, O., and Babior, B.M. (1998) Activation of p47(PHOX), a cytosolic subunit of the leukocyte NADPH oxidase. Phosphorylation of ser-359 or ser-370 precedes phosphorylation at other sites and is required for activity. *J. Biol. Chem.* **273**, 35147–35152
12. Inanami, O., Yamamori, T., Takahashi, T.A., Nagahata, H., and Kuwabara, M. (2001) ESR detection of intraphagosomal superoxide in polymorphonuclear leukocytes using 5-(diethoxyphosphoryl)-5-methyl-l-pyrroline-N-oxide. *Free Radic. Res.* **34**, 81–92
13. Yoshida, L.S., Abe, S., and Tsunawaki, S. (2000) Fungal gliotoxin targets the onset of superoxide-generating NADPH oxidase of human neutrophils. *Biochem. Biophys. Res. Commun.* **268**, 716–723
14. Tsunawaki, S., Yoshida, L.S., Nishida, S., Kobayashi, T., and Shimoyama, T. (2004) Fungal metabolite gliotoxin inhibits assembly of the human respiratory burst NADPH oxidase. *Infect. Immun.* **72**, 3373–3382
15. Nishida, S., Yoshida, L.S., Shimoyama, T., Nunoi, H., Kobayashi, T., and Tsunawaki, S. (2005) Fungal metabolite gliotoxin targets flavocytochrome b558 in the activation of the human neutrophil NADPH oxidase. *Infect. Immun.* **73**, 235–244
16. Nakashima, T., Kurachi, M., Kato, Y., Yamaguchi, K., and Oda, T. (2005) Characterization of bacterium isolated from the sediment at coastal area of Omura Bay in Japan and several biological activities of pigment produced by this isolate. *Microbiol. Immunol.* **49**, 407–415
17. Nakashima, T., Tamura, T., Kurachi, M., Yamaguchi, K., and Oda, T. (2005) Apoptosis-mediated cytotoxicity of prodigiosin-like red pigment produced by gamma-Proteobacterium and its multiple bioactivities. *Biol. Pharm. Bull.* **28**, 2289–2295
18. Nakashima, T., Miyazaki, Y., Matsuyama, Y., Muraoka, W., Yamaguchi, K., and Oda, T. (2006) Producing mechanism of an algicidal compound against red tide phytoplankton in a marine bacterium gamma-proteobacterium. *Appl. Microbiol. Biotechnol.* **73**, 684–690
19. Gerber, N.N. (1975) Prodigiosin-like pigments. *CRC. Crit. Rev. Microbiol.* **3**, 469–485
20. Campàs, C., Dalmau, M., Montaner, B., Barragán, M., Bellosillo, B., Colomer, D., Pons, G., Pérez-Tomás, R., and Gil, J. (2003) Prodigiosin induces apoptosis of B and T cells from B-cell chronic lymphocytic leukemia. *Leukemia* **17**, 746–750
21. Diaz-Ruiz, C., Montaner, B., and Perez-Tomas, R. (2001) Prodigiosin induces cell death and morphological changes indicative of apoptosis in gastric cancer cell line HGT-1. *Histol. Histopathol.* **16**, 415–421
22. Castro, A.J. (1967) Antimalarial activity of prodigiosin. *Nature* **213**, 903–904
23. Gerber, N.N. (1975) A new prodiginne (prodigiosin-like) pigment from Streptomyces. Antimalarial activity of several prodiginnes. *J. Antibiot. (Tokyo)* **28**, 194–199
24. Gerber, N.N. (1971) Prodigiosin-like pigments from Actinomadura (Nocardia) pelletieri. J. Antibiot. (Tokyo) **24**, 636–640

25. Nakashima, T., Kato, Y., Yamaguchi, K., and Oda, T. (2005) Evaluation of the anti-Trichophyton activity of a prodigiosin analogue produced by gamma-proteobacterium, using stratum corneum epidermis of the Yucatan micropig. *J. Infect. Chemother.* **11**, 123–128
26. Mortellaro, A., Songia, S., Gnocchi, P., Ferrari, M., Fornasiero, C., D'Alessio, R., Isetta, A., Colotta, F., and Golay, J. (1999) New immunosuppressive drug PNU156804 blocks IL-2-dependent proliferation and NF-kappa B and AP-1 activation. *J. Immunol.* **162**, 7102–7109
27. D'Alessio, R., Bargiotti, A., Carlini, O., Colotta, F., Ferrari, M., Gnocchi, P., Isetta, A., Mongelli, N., Motta, P., Rossi, A., Rossi, M., Tibolla, M., and Vanotti, E. (2000) Synthesis and immunosuppressive activity of novel prodigiosin derivatives. *J. Med. Chem.* **43**, 2557–2565
28. Melvin, M.S., Calcutt, M.W., Noftle, R.E., and Manderville, R.A. (2002) Influence of the a-ring on the redox and nuclease properties of the prodigiosins: importance of the bipyrrole moiety in oxidative DNA cleavage. *Chem. Res. Toxicol.* **15**, 742–748
29. Imada, I., Sato, E.F., Miyamoto, M., Ichimori, Y., Minamiyama, Y., Konaka, R., and Inoue, M. (1999) Analysis of reactive oxygen species generated by neutrophils using a chemiluminescence probe L-012. *Anal. Biochem.* **271**, 53–58
30. Woodman, R.C., Ruedi, J.M., Jesaitis, A.J., Okamura, N., Quinn, M.T., Smith, R.M., Curnutte, J.T., and Babior, B.M. (1991) Respiratory burst oxidase and three of four oxidase-related polypeptides are associated with the cytoskeleton of human neutrophils. *J. Clin. Invest.* **87**, 1345–1351
31. Li, J.M. and Shah, A.M. (2002) Intracellular localization and preassembly of the NADPH oxidase complex in cultured endothelial cells. *J. Biol. Chem.* **277**, 19952–19960
32. Lowry, O.H., Rosbrough, N.J., Farr, A.L., and Randal, R.J. (1951) Protein measurement with the Folin phenol reagent. *J. Biol. Chem.* **193**, 265–275
33. Li, J.M. and Shah, A.M. (2002) Intracellular localization and preassembly of the NADPH oxidase complex in cultured endothelial cells. *J. Biol. Chem.* **277**, 19952–19960
34. Cushley, R.J., Sykes, R.J., Shaw, C-K., and Wasserman, H.H. (1975) Carbon-13 fourier transform nuclear magnetic resonance. IX. Complete assignments of some prodigiosins. Bioincorporation of label. *Can. J. Chem.* **53**, 148–160
35. Nauseef, W.M., Volpp, B.D., McCormick, S., Leidal, K.G., and Clark, R.A. (1991) Assembly of the neutrophil respiratory burst oxidase. Protein kinase C promotes cytoskeletal and membrane association of cytosolic oxidase components. *J. Biol. Chem.* **266**, 5911–5917
36. Clark, R.A., Volpp, B.D., Leidal, K.G., and Nauseef, W.M. (1990) Two cytosolic components of the human neutrophil respiratory burst oxidase translocate to the plasma membrane during cell activation. *J. Clin. Investig.* **85**, 714–721
37. Tsunawaki, S., Mizunari, H., Namiki, H., and Kuratsuji, T. (1994) NADPH-binding component of the respiratory burst oxidase system: studies using neutrophil membranes from patients with chronic granulomatous disease lacking the beta-subunit of cytochrome b558. *J. Exp. Med.* **179**, 291–297
38. Babior, B.M. (2004) NADPH oxidase. *Curr. Opin. Immunol.* **16**, 42–47
39. Nakashima, T., Kim, D., Miyazaki, Y., Yamaguchi, K., Takeshita, S., and Oda, T. (2006) Mode of action of an antialgal agent produced by a marine gammaproteobacterium against *Chattonella marina*. *Aquat. Microb. Ecol.* **452**, 55–262
40. Das, K.C. and Misra, H.P. (1994) Impairment of raw 264.7 macrophage function by antiarrhythmic drugs. *Mol. Cell Biochem.* **30**, 151–62
41. Combadiere, C., Hakim, J., Giroud, J.P., and Perianin, A. (1990) Staurosporine, a protein kinase inhibitor, up-regulates the stimulation of human neutrophil respiratory burst by N-formyl peptides and platelet activating factor. *Biochem. Biophys. Res. Commun.* **168**, 65–70
42. Kanai, F., Liu, H., Field, S.J., Akbary, H., Matsuo, T., Brown, G.E., Cantley, L.C., and Yaffe, M.B. (2001) he PX domains of p47phox and p40phox bind to lipid products of PI(3)K. *Nat. Cell. Biol.* **3**, 675–678
43. Bravo, J., Karathanassis, D., Pacold, C.M., Pacold, M.E., Ellson, C.D., Anderson, K.E., Butler, P.J., Lavenir, I., Perisic, O., Hawkins, P.T., Stephens, L., and Williams, R.L. (2001) The crystal structure of the PX domain from p40phox bound to phosphatidylinositol 3-phosphate. *Mol. Cell* **8**, 829–839
44. Kuribayashi, F., Nunoi, H., Wakamatsu, K., Tsunawaki, S., Sato, K., Ito, T., and Sumimoto, H. (2002) The adaptor protein p40(phox) as a positive regulator of the superoxide-producing phagocyte oxidase. *EMBO J.* **21**, 6312–6320
45. Ueyama, T., Tatsuno, T., Kawasaki, T., Tsujibe, S., Shirai, Y., Sumimoto, H., Leto, T.L., and Saito, N. (2007) A regulated adaptor function of p40phox: distinct p67phox membrane targeting by p40phox and by p47phox. *Mol. Biol. Cell.* **18**, 441–454
46. Chuang, T.H., Bohl, B.P., and Bokoch, G.M. (1993) *J. Biol. Chem.* **268**, 26206–26211
47. Quinn, M.T., Evans, T., Loetterle, L.R., Jesaitis, A.J., and Bokoch, G.M. (1993) Guanine nucleotide exchange regulates membrane translocation of Rac/Rho GTP-binding proteins. *J. Biol. Chem.* **268**, 20983–20987
48. Abo, A., Webb, M.R., Grogan, A., and Segal, A.W. (1994) Activation of NADPH oxidase involves the dissociation of p21rac from its inhibitory GDP/GTP exchange protein (rhoGDI) followed by its translocation to the plasma membrane. *Biochem. J.* **298**, 585–591
49. Koga, H., Terasawa, H., Nunoi, H., Takeshige, K., Inagaki, F., and Sumimoto, H. (1999) Tetratricopeptide repeat (TPR) motifs of p67(phox) participate in interaction with the small GTPase Rac and activation of the phagocyte NADPH oxidase. *J. Biol. Chem.* **274**, 25051–25060
50. Lapouge, K., Smith, S.J., Walker, P.A., Gamblin, S.J., Smerdon, S.J., and Rittinger, K. (2000) Structure of the TPR domain of p67phox in complex with Rac. GTP. *Mol. Cell.* **6**, 899–907
51. Dang, P.M., Cross, A.R., Quinn, M.T., and Babior, B.M. (2002) Assembly of the neutrophil respiratory burst oxidase: a direct interaction between p67PHOX and cytochrome b558 II. *Proc. Natl. Acad. Sci. USA* **99**, 4262–4265
52. Bokoch, G.M. (1995) Regulation of the phagocyte respiratory burst by small GTP-binding proteins. *Trends Cell. Biol.* **5**, 109–113